ORIGINAL ARTICLE

A novel *TRAPPC11* mutation in two Turkish families associated with cerebral atrophy, global retardation, scoliosis, achalasia and alacrima

Katrin Koehler,[1] Miroslav P. Milev,[2] Keshika Prematilake,[2] Felix Reschke,[1] Susann Kutzner,[1] Ramona Jühlen,[1] Dana Landgraf,[1] Eda Utine,[3] Filiz Hazan,[4] Gulden Diniz,[5] Markus Schuelke,[6] Angela Huebner,[1] Michael Sacher[2,7]

► Additional material is published online only. To view please visit the journal online (http://dx.doi.org/10.1136/jmedgenet-2016-104108)

For numbered affiliations see end of article.

Correspondence to
Dr Katrin Koehler, Division of Paediatric Endocrinology and Diabetology, Department of Paediatrics, Clinical Research, Technical University Dresden, Fetscherstrasse 74, 01307 Dresden, Germany; katrin.koehler@uniklinikum-dresden.de

KK, MPM and KP contributed equally.

Received 16 June 2016
Revised 02 September 2016
Accepted 10 September 2016
Published Online First
5 October 2016

ABSTRACT

Background Triple A syndrome (MIM #231550) is associated with mutations in the *AAAS* gene. However, about 30% of patients with triple A syndrome symptoms but an unresolved diagnosis do not harbour mutations in *AAAS*.

Objective Search for novel genetic defects in families with a triple A-like phenotype in whom *AAAS* mutations are not detected.

Methods Genome-wide linkage analysis, whole-exome sequencing and functional analyses were used to discover and verify a novel genetic defect in two families with achalasia, alacrima, myopathy and further symptoms. Effect and pathogenicity of the mutation were verified by cell biological studies.

Results We identified a homozygous splice mutation in *TRAPPC11* (c.1893+3A>G, [NM_021942.5], g.4:184,607,904A>G [hg19]) in four patients from two unrelated families leading to incomplete exon skipping and reduction in full-length mRNA levels. *TRAPPC11* encodes for trafficking protein particle complex subunit 11 (TRAPPC11), a protein of the transport protein particle (TRAPP) complex. Western blot analysis revealed a dramatic decrease in full-length TRAPPC11 protein levels and hypoglycosylation of LAMP1. Trafficking experiments in patient fibroblasts revealed a delayed arrival of marker proteins in the Golgi and a delay in their release from the Golgi to the plasma membrane. Mutations in *TRAPPC11* have previously been described to cause limb-girdle muscular dystrophy type 2S (MIM #615356). Indeed, muscle histology of our patients also revealed mild dystrophic changes. Immunohistochemically, β-sarcoglycan was absent from focal patches.

Conclusions The identified novel *TRAPPC11* mutation represents an expansion of the myopathy phenotype described before and is characterised particularly by achalasia, alacrima, neurological and muscular phenotypes.

INTRODUCTION

Triple A syndrome (MIM #231550) is an autosomal recessive disease characterised by adrenocorticotropic hormone-resistant adrenal insufficiency, achalasia and alacrima.[1] In addition to the three main features, patients often present with a variety of dermatological features and progressive neurological symptoms involving the central, peripheral and autonomic nervous systems. Some patients also display intellectual disabilities. The phenotype is highly variable with regard to severity, age of onset and manifestation of all main symptoms. In addition, adrenal failure may occur later in life or may not arise at all.[2] Classical triple A syndrome is caused by homozygous or compound heterozygous mutations in the achalasia-addisonianism-alacrima syndrome (*AAAS*) gene on chromosome 12q13.[3 4] This gene encodes a protein of the nuclear pore complex (NPC) named ALADIN (ALacrima Achalasia aDrenal Insufficiency Neurologic disorder).[5] While most ALADIN mutants fail to localise to the NPC,[6 7] mutations in this protein result in dysregulation of cellular redox homeostasis in vitro, suggesting a role in the progressive degeneration of affected tissues.[8 9]

Recently, a triple A-like disease, the alacrima, achalasia and mental retardation (AAMR) syndrome (MIM #615510) was described to be caused by mutations in the GDP-mannose pyrophosphorylase A (*GMPPA*) gene on chromosome 2q35.[10] These patients presented at birth or in the first years of life with alacrima, achalasia and psychomotor developmental delay with speech delay, but without clinical symptoms of adrenal insufficiency. Most patients also had muscular hypotonia and share aspects with hereditary sensory and autonomic neuropathies.[10] Although the underlying cellular mechanism of GMPPA dysfunction is not fully known, a loss of function of GDP-mannose pyrophosphorylase, consisting of the regulatory subunit GMPPA and the catalytic subunit GMPPB, is assumed.[10] Interestingly, about 30% of the patients with a suspected triple A syndrome due to a combination of typical symptoms do not harbour any mutations in *AAAS* or *GMPPA* suggesting that triple A syndrome is a genetically heterogeneous disorder.[11] To date, the intriguing combination of achalasia and alacrima is caused only by mutations in *AAAS* or *GMPPA*, whereby hitherto the specific mechanism is obscure. It is assumed that neural degeneration plays a role.

Muscular dystrophy encompasses a large group of muscular disorders with limb-girdle muscular dystrophies (LGMD) accounting for up to one-third of muscular dystrophy cases. The LGMD phenotype has been associated with mutations in 30 different protein-coding genes.[12] The combination of myopathy with mental retardation occurs more frequently in muscular dystrophy–dystroglycanopathy

To cite: Koehler K, Milev MP, Prematilake K, *et al. J Med Genet* 2017;**54**:176–185.

(MDDG), for example, MDDGB1 (*POMT1*), MDDGB2 (*POMT2*), MDDGB3 (*POMGNT1*), MDDGB5 (*FKRP*), MDDGB6 (*LARGE*) and MDDGB14 (*GMPPB*) mostly affecting O-mannosyl glycosylation of dystroglycans.[13–19] There are overlapping phenotypes, for example, mutations in *GMPPB* also cause LGMD2T with mental retardation.[19]

Here, we report the discovery of a novel mutation in the trafficking protein particle complex subunit 11 (*TRAPPC11*) gene in two unrelated consanguineous Turkish families each with two patients suffering from myopathy and intellectual disability including cerebral atrophy, scoliosis, achalasia and alacrima, thus expanding the clinical phenotype of *TRAPPC11* mutations.

PATIENTS

The study was approved by the local ethics review board (Medical Faculty, Technical University Dresden; EK820897). All subjects or their legal representatives gave written informed consent to the study. The study was performed in accordance with the Declaration of Helsinki. The two unrelated consanguineous families (F1 and F2) originated from Turkey. The parents are each first-degree cousins. An overview of the symptoms of all patients is given in table 1. Patients' case presentations are reported in detail in the online supplementary information section.

MATERIALS AND METHODS

Homozygosity mapping

Blood samples from patients for DNA analysis were collected after obtaining written informed consent. DNA preparation was performed according to standard protocols using the QIAamp DNA Mini Kit (Qiagen). Homozygosity mapping was done with DNA samples of three affected patients of both families (F1.II:2, F2.II:2, F2.II:3) using the GeneChip Human Mapping 6.0 SNP array (Affymetrix), as described.[20] HomozygosityMapper 2012 (http://www.homozygositymapper.org) was used to delineate genetic intervals that were homozygous for 400 SNPs in succession in the affected individuals.[21] Both families were analysed separately.

Table 1 Clinical presentation of the affected individuals

Patient	F1.II:1	F1.II:2	F2.II:2	F2.II:3
Consanguinity	Yes	Yes	Yes	Yes
Sex	Male	Female	Male	Female
Age	16	12	15	13
Cardinal symptoms of triple A syndrome				
Achalasia	Yes	No	Yes	Yes
Achalasia age of onset (years)	0.5	–	2.5	2
Alacrima	Yes	Yes	Yes	Yes
Alacrima age of onset (years)	Birth	0.5	Birth	Birth
Adrenal insufficiency	No	No	No	No
Epidermal symptoms				
Hyperkeratosis	Yes	Yes	No	No
Neurological and muscular symptoms				
Intellectual disability	Yes	Yes	Yes	Yes
Milestones delay	Yes	Yes	Yes	Yes
Muscular weakness/dystrophy	Weakness	Weakness	Dystrophy	Atrophy
Gait abnormalities	Yes	No gait	No gait	No gait
Cerebral atrophy in MRI	Yes	Yes	Yes	Yes
Speech delay (few words)	Yes	Yes	Yes	Yes
Nasal speech	No	Yes	No	No
Other symptoms				
Short stature	Yes	Yes	Yes	Yes
Dystrophy: body weight <10 percentile	Yes	Yes	Yes	Yes
Epilepsy/seizures	Yes	Yes	–	–
Caries	Yes	Yes	No	No
Nephrolithiasis	Yes	No	No	No
Undescended testis	Yes	–	No	–
Scoliosis	Yes	Yes	Yes	Yes

Whole exome sequencing

Exonic sequences were enriched from patient F2.II:2 using NimbleGen SeqCap EZ human exome library V.2.0 and sequenced on a HiSeq2000 (Illumina) with read length of paired-end 2× 100 bp and average coverage of >50-fold. FASTQ files (FASTA format sequences bundled with their quality data) were aligned to the human GRCh37.p11 (hg19) reference sequence using the BWA-MEM V.0.7.1 aligner. A variant file was generated for all exons ±20 bp flanking regions using the GATK V.3.3 software package and sent to MutationTaster2 (http://www.mutationtaster.org) for the assessment of potential pathogenicity.[22] Filtering options were used as described.[20] All relevant variants were inspected visually using the Integrative Genomics Viewer (http://www.broadinstitute.org/igv).

Sanger sequencing and microsatellite analysis

Cosegregations of the *TRAPPC11* mutation in families F1 and F2 were verified by automatic Sanger sequencing using an ABI 3130xL genetic analyser and BigDye Terminator Cycle Sequencing Kit 1.1 (Applied Biosystems). Exon 18 and flanking intronic regions were amplified with primer pair 5′-TAA GTG CAG AAG TCA GTA AGA ATG-3′ and 5′-ATT TGT TAC TAT GAA ACC ATT AAG AC-3′. Primer pairs for sequencing of coding regions and all exon/intron junctions of the *TRAPPC11* gene are listed in online supplementary table S1.

Haplotype analysis was performed with M13-labelled primers by standard semi-automated methods using an ABI 3130xL Genetic Analyzer.[23] Marker information and primer sequences are listed in online supplementary tables S2 and S3. Allele calling was performed using GeneScan Software, V.3.7.1 and GeneMapper 4.0 (Applied Biosystems).

RT-PCR analysis

Total RNA from blood was collected into a PAXgene Blood RNA Tube (BD) and prepared using PAXgene Blood RNA Kit (Qiagen). After reverse transcription of messenger RNA (mRNA) with Go Script Reverse Transcription System (Promega), the sequences of exons 17–19 of *TRAPPC11* were amplified using the following primers: 5′-ATG AAA GTC CTG ATC CAG AAC-3′ (forward primer exon 17) and 5′-GGC ACA TCT TTC CTT GAG TC-3′ (reverse primer exon 19).

Fibroblast RNA was isolated using the Nucleospin RNAII kit (Macherey-Nagel) with on-column DNase treatment. Quantitative RT-PCR on cDNA from patients (F1.II:1, F1.II:2, F2.II:3) and two control fibroblasts were set up in triplicates from three independent RNA preparations per sample on a 7300 Real-Time PCR system (ABI) using GoTaq Probe qPCR Master Mix (Promega). Sequences of the wild-type *TRAPPC11* allele (exons 17–18) were amplified using oligonucleotide primers 5′-GCT GTG AAA ACT GCT CAG AAG CT-3′ (forward primer exon 17), 5′-GGC TTT GCA CTG CAC AAA TG-3′ (reverse primer exon 17/18) and probe 5′-FAM TTT CTC TGG CTG GCA GCA ATA TTT TCA CAA TAMRA-3′ (exon 17). Sequences of the mutant *TRAPPC11* allele (exons 17–19 without exon 18)

were amplified in a second reaction using the same forward primer and probe from exon 17 and an artificial reverse primer Ex17/19-R 5′-CAG AAC TGG TTG TAT TCC AAA TGG-3′. Gene transcription was normalised in relation to the transcription of the housekeeping gene β-actin with the following primers: 5′-GCA CCC AGC ACA ATG AAG ATC-3′, 5′-CGC AAC TAA GTC ATA GTC CGC-3′ and the β-actin-probe 5′-FAM TGC TCC TCC TGA GCG CAA GTA CTC C TAMRA-3′.

Western blot

Lysates of cultured fibroblasts from control individuals or patients were prepared by harvesting cells in lysis buffer (20 mM HEPES, pH 7.4, 0.1 M KCl, 0.5% Triton X-100, 5 mM $MgCl_2$ with protease inhibitors). A total of 30 µg of protein was fractionated on an sodium dodecyl sulfate (SDS)–polyacrylamide gel. The fractionated proteins were transferred to a nitrocellulose membrane, blocked for 1 hour with 5% skim milk in 1× PBS-T (PBS with 0.1% Tween 20) and then incubated for 1 hour with primary antibody. The primary antibodies used were anti-green fluorescence protein (GFP) (Roche), anti-tubulin (Sigma), anti-LAMP1 (H4A3, Santa Cruz Biotechnology) and anti-TrappC11.[24] The appropriate secondary antibodies (anti-rabbit-horseradish peroxidase (HRP) or anti-mouse-HRP) (KPL) were then added in 1× PBS-T for 45 min. After washing the membrane, the signal was developed using enhanced chemiluminescence (ECL) western blotting detection reagents (GE Amersham) and visualised on a GE Amersham Imager 600.

VSVG–GFP ts045 assay

Fibroblast cells were infected with virus encoding vesicular stomatitis virus glycoprotein (VSVG)–GFP ts045 for 1 hour at 37°C. The cells were then incubated for ∼18 hours at 40°C. Prior to a shift to 32°C, cycloheximide was added to a final concentration of 10 µg/mL. At various time points, cells were either fixed in 3% paraformaldehyde for 20 min and processed for immunofluorescence microscopy (see below) or quickly harvested in ice-cold lysis buffer (20 mM HEPES, pH 7.4, 0.1 M KCl, 0.5% Triton X-100, 5 mM $MgCl_2$ with protease inhibitors). For endoglycosidase H (endo H) treatment, 5–20 µg of total cell lysate was denatured at 100°C for 10 min before the addition of 10 U of endo H. Treated samples were incubated for 1 hour at 37°C. Western blot analysis was used to detect the fusion protein using mouse anti-GFP (Roche). Quantitation of western blots scanned on a GE Amersham Imager 600 was performed using the ImageJ V.1.48 program (National Institutes of Health (NIH)) after background subtraction and are expressed as endo H-resistant pixels/(endo H-resistant + endo H-sensitive pixels) at each time point.

Fluorescence microscopy

Following fixation in paraformaldehyde, samples for immunofluorescence microscopy were first quenched with 0.1 M glycine for 10 min, permeabilised in 0.2% Triton X-100 for 5 min and then blocked with 5% normal goat serum (NGS, Cell Signaling Technology) for 40 min. Primary (mouse antibody anti-GFP (Sigma) and rabbit anti-mannosidase II (kind gift from Kelley Moreman, University of Georgia)) were diluted in 5% NGS and incubated overnight at 4°C. After washing with PBS, secondary antibodies (antimouse AlexaFluor-488 and antirabbit AlexaFluor-647) and DAPI were applied for 1 hour at room temperature. Images of 1024×1024 pixel resolution were captured on a Nikon C2 laser scanning confocal microscope fitted with a 63× Plan Apo I, NA1.4 objective (Nikon) controlled by NIS Elements C 4.4 software. Optical sections of 0.2 µm increments were acquired.

Time-lapse microscopy

Fibroblast cells were treated as described for the VSVG–GFP assay except they were plated on glass-bottom dishes (14 mm diameter, thickness of 1.5; MatTek). Immediately after the 40°C incubation, the dishes were placed in the temperature-controlled chamber of the microscope heated to 32°C with 5% CO_2. Time-lapse microscopy was performed beginning at 3 min after the temperature shift (a time necessary to select the cells for imaging) using a 40× oil objective (NA 1.3), no binning, on an inverted confocal microscope (LiveScan Swept Field; Nikon), Piezo Z stage (Nano-Z100N; Mad City Labs) and an electron-multiplying charge-coupled device camera (512×512, iXon X3; Andor Technology). Images were acquired with NIS-Elements V.4.0 acquisition software every 30 s using a 0.7 s exposure at 0.2 µm increments with a slit size of 50 µm for up to 3 hours. Images were viewed and analysed on ImageJ V.1.48 (NIH). Montages of images from the videos with corresponding time points were plotted in Illustrator CS6 (Adobe).

Immunohistochemistry

Muscle biopsy was performed on patient F2.II:3. The muscle biopsy sample from the gastrocnemius muscle was frozen in isopentane precooled in liquid nitrogen and 8–12 µm sections were cut using a cryostat. These sections were stained with routine histochemical and enzyme histochemical stains, such as H&E, modified Gomori's trichrome and Masson's trichrome. A rich panel of antibodies against structural proteins of muscle fibre was performed immunohistochemically. These included antispectrin (Novocastra, NCL-spec1), antidystrophin N-terminus (Novocastra, NCL-dys3), antiadhalin (Novocastra, NCL-α-sarc) and other antisarcoglycans (Novocastra, NCL-β–δ–γ-sarc) antibodies. In addition, antimyosin heavy chain fast and slow (Novocastra, NCL-MHCf/MHCs) antibodies were used for discriminating between fibre type, and antimyosin heavy chain neonatal (Novocastra, NCL-MHCn) antibody was used for identification of pathological immature fibres.

Statistical analyses

All data sets were shown as means±SEM. Statistical significance was assessed using an unpaired two-tailed Student's t-test using the GraphPad Prism software statistical package 6.0 (GraphPad Software). The significance level was set to $p<0.05$.

RESULTS

Molecular genetics

In the present study, we investigated two consanguineous Turkish families (F1 and F2) each with two affected siblings, who suffer from a triple A-like syndrome with alacrima and achalasia, but without signs of adrenal insufficiency (for laboratory findings, see online supplementary table S4). The parents and three siblings were unaffected, consistent with an autosomal-recessive mode of inheritance. Autozygosity mapping delineated various regions in both families (see online supplementary figures S2 and S3 and table S5), but only one region of 2.7 Mbp on chromosome 4 that was shared by both families and that was flanked by the SNPs rs6854653 and rs9685847 (figure 1A). Whole exome sequencing was performed on patient F2.II:2. In order to identify the common disease gene for both families as well as further potential disease-causing mutations in other genes that were only located in the autozygous regions of family 2 in the potential case of a

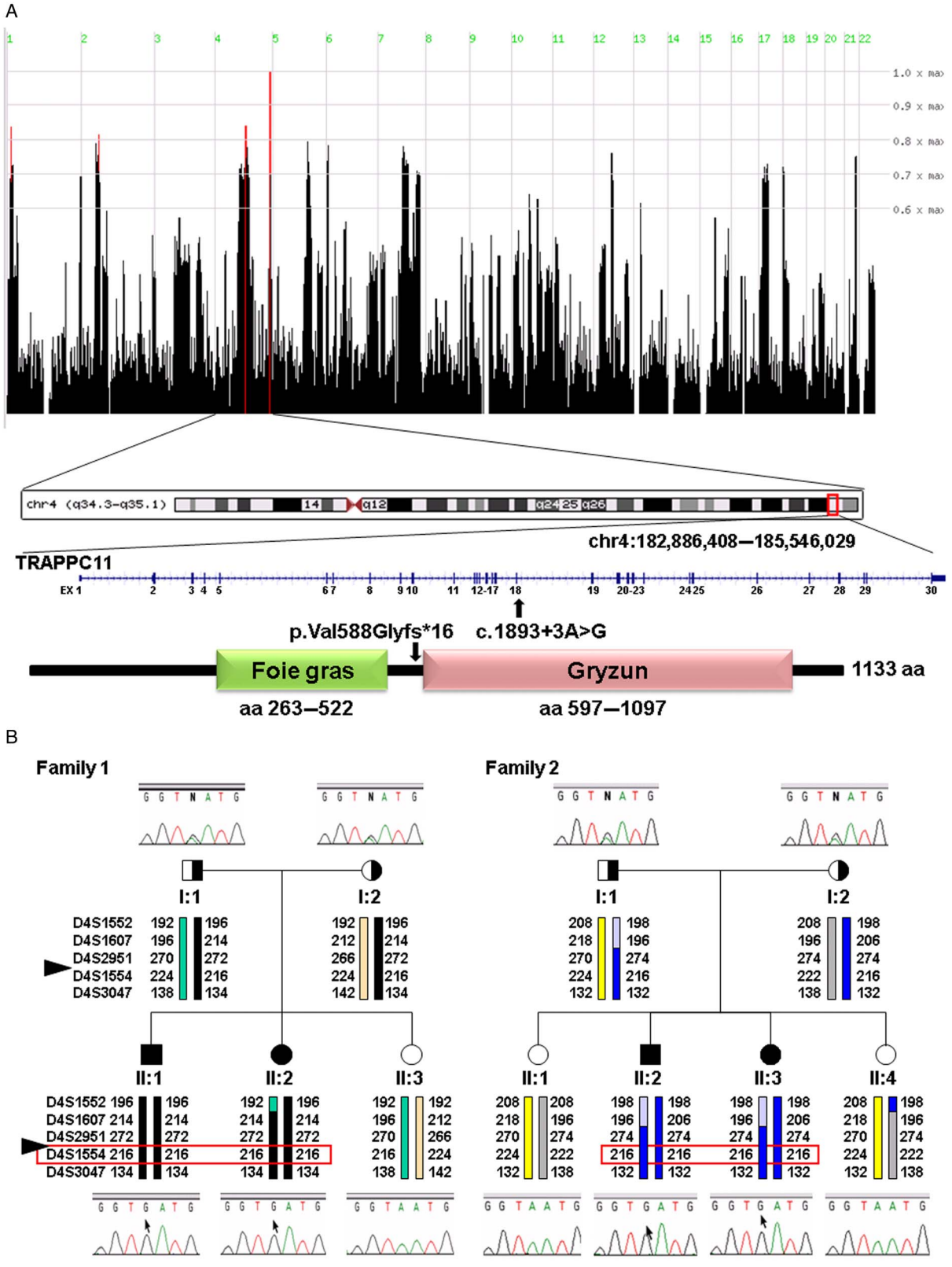

Figure 1 Affected individuals carry a homozygous trafficking protein particle complex subunit 11 (*TRAPPC11*) mutation. (A) HomozygosityMapper2012 analysis revealed one locus on chromosome 4 with the highest score that was homozygous in all three investigated patients. This locus comprised 2.7 Mbp and covered 30 protein-coding genes. The *TRAPPC11* gene is located among them, and the identified DNA alteration and the predicted change at the protein level is indicated. (B) Haplotype analysis using microsatellite markers of the chromosomal *TRAPPC11* region revealed a shared haplotype of the *TRAPPC11* flanking marker D4S1554 (highlighted by the red square). The sequencing electropherograms at the genomic DNA level of all family members shows the segregation of the mutation in both families.

two-gene disorder,[25] we subjected all variants found in all the autozygous regions (corresponding to 548 protein-coding genes) to a MutationTaster2 analysis. Using this approach, we only identified a single homozygous variant in *TRAPPC11* (c.1893+3A>G, [NM_021942.5], g.4:184,607,904A>G [hg19]) at the splice donor site of exon 18 that was predicted to affect splicing. The coverage of this position was 132×. The variant was neither listed in the 1000 genome (http://www.1000genomes.org) nor in the 5000 exome (https://http://www.genomeweb.com/sequencing/baylor-sequence-more-5000-exomes-human-disease-studies) projects or in the dbSNP (http://www.ncbi.nlm.nih.gov/SNP) and Exome Aggregation Consortium (ExAC) databases (http://exac.broadinstitute.org). The genotype–phenotype segregation in the family was verified by Sanger sequencing. The same mutation could be identified in the second apparently unrelated family (F1), which also segregated with the phenotype (figure 1B). Having identified the mutation in *TRAPPC11* as the likely underlying genetic defect in these two families, we screened 56 additional patients affected by triple A syndrome or a triple A-like disorder. These patients were selected since they carry no mutation in *AAAS* or *GMPPA*. None of these patients revealed a *TRAPPC11* mutation in any of the 29 coding exons (exons 2–30) and exon–intron boundaries.

To clarify whether the two families would be closely related, we performed a haplotype analysis using microsatellite markers of the chromosomal *TRAPPC11* region. We found a shared haplotype of the *TRAPPC11* flanking marker *D4S1554* in families F1 and F2 (figure 1B). In the affected patients of family F1, we found a homozygous haplotype over nearly the entire region. Although the two patients of family F2 show a homozygous region around the *TRAPPC11* gene, they shared only one flanking microsatellite marker with family F1, indicating that the families are not closely related but the mutation might be a founder mutation.

Consequences of the *TRAPPC11* mutation on the transcript level

The c.1893+3A>G mutation was further qualitatively and quantitatively investigated on the mRNA level. After amplification of exon 17 to exon 19 of reverse transcribed *TRAPPC11* mRNA from patients F1.II:1 and F1.II:2, we found that patient cells produced an out-of-frame aberrant splice product in which the 131 bp of exon 18 is missing. Patient cells also produced the regular splice product that includes exon 18 (figure 2A). Quantitative measurements (qRT-PCR with TaqMan) revealed that patient fibroblasts had only 20% of the regular splice product as compared with control fibroblasts (100%) (figure 2B), suggesting an incomplete splicing defect due to the mutation. The aberrant splice product of patient cells was calculated to be only about 12% of the quantity in comparison with the regular splicing product of the control cells. From this, we conclude that a loss of 80% of the intact *TRAPPC11* transcripts in combination with an aberrant splicing product causes the phenotype of the patients. Quantitative measurements of mRNA from parent's blood cells revealed comparable levels of the regular splice product in heterozygous carriers of the c.1893+3A>G mutation compared with controls without this mutation. The levels of the aberrant splice product were only about half as high as those of the homozygotes (see online supplementary figure S4).

Western blot analysis of TRAPPC11 and LAMP1

We next sought to determine the consequences on the cellular level of the c.1893+3A>G mutation. The splicing defect that deletes exon 18 is predicted to result in the mutant protein p.Val588Glyfs16*, resulting in a truncation of the protein just prior to the conserved gryzun domain (figure 1A). Lysates prepared from fibroblasts derived from two affected individuals (F1.II:1 and F1.II:2) were subjected to western blot analysis using rabbit antiserum raised against the human TRAPPC11 protein[24] and against the human LAMP1 protein. Since this TRAPPC11 antiserum was raised against an epitope in the extreme carboxy portion of the protein, a truncated product, as expected for this mutation, would not be detected. Rather, we detected a dramatic decrease in the levels of full-length TRAPPC11 in both affected individuals (figure 3A). Small amounts of full-length TRAPPC11 in the lysates from the affected individuals are consistent with the incomplete splicing

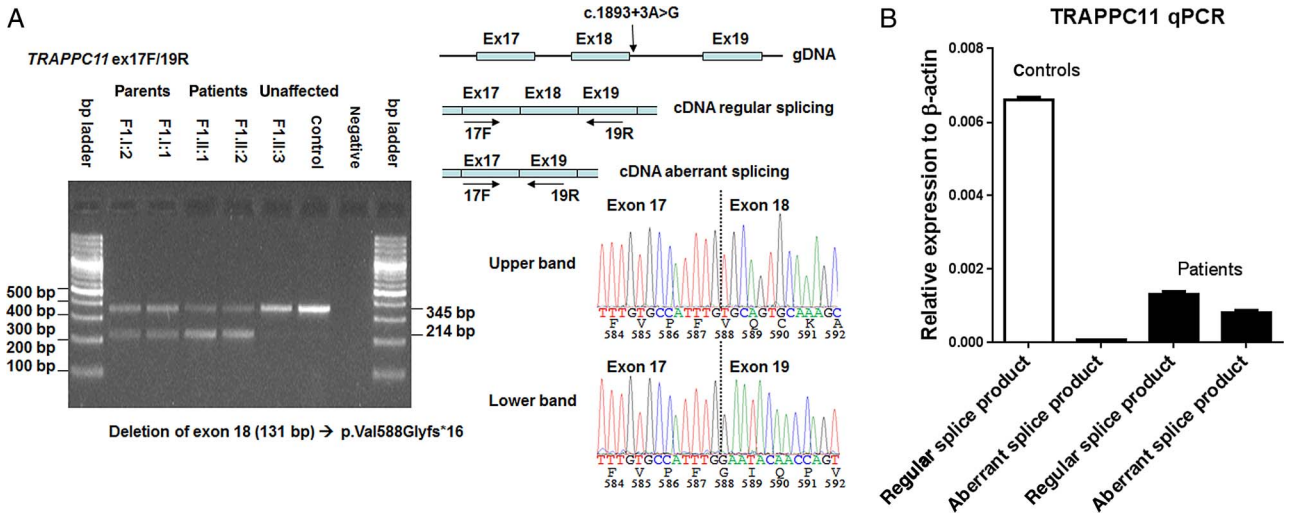

Figure 2 Affected individuals have reduced levels of trafficking protein particle complex subunit 11 (TRAPPC11) transcript as well as a novel splice variant. (A) Agarose gel electrophoresis and sequencing chromatograms of cDNA-derived PCR products using PAXgene blood RNA and primers amplifying exons 17–19. PCR-amplified cDNA fragments were analysed by electrophoresis on a 2% agarose gel and by sequencing. The 345 bp amplicon represents the regular splice product and the 214 bp amplicon represents the aberrant splicing product; control=pooled cDNA; negative=water control. (B) *TRAPPC11* mRNA-expression analysis performed by TaqMan PCR on fibroblast cDNA. A reduction of ~80% *TRAPPC11* expression in affected individuals compared with control was shown.

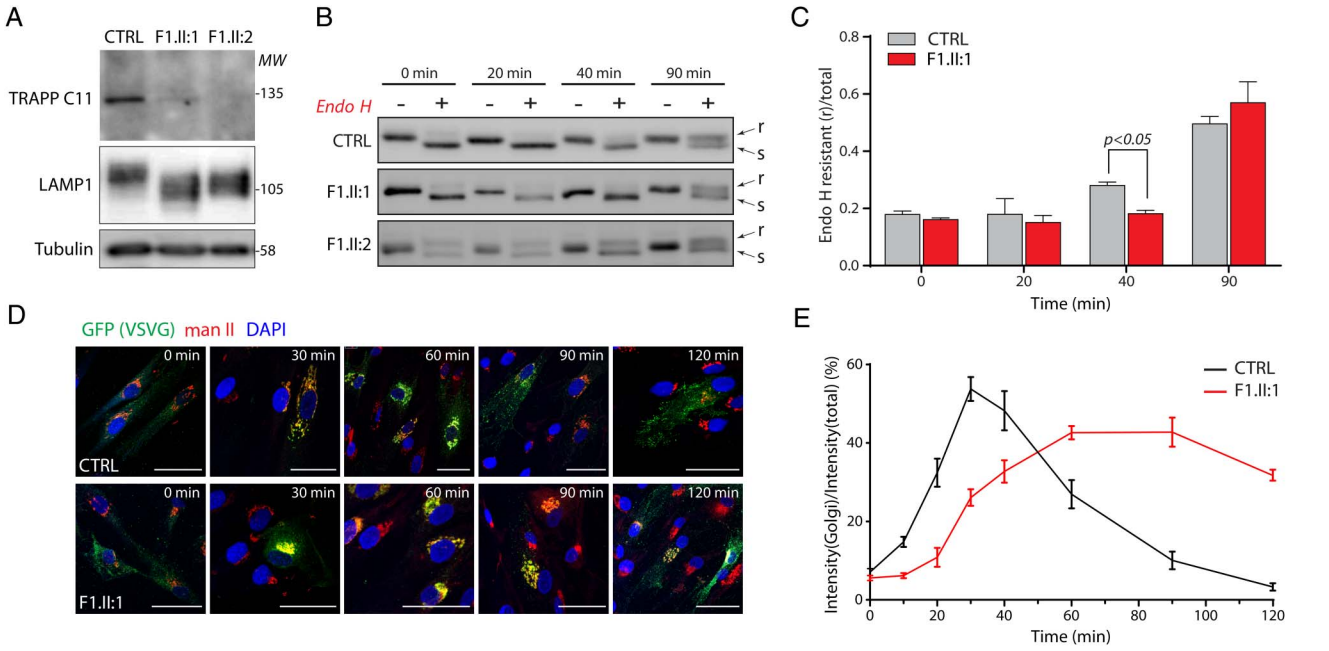

Figure 3 The affected individuals showed a delay in endoglycosidase H resistance and an accumulation of vesicular stomatitis virus glycoprotein (VSVG)–GFP ts045 in the Golgi. (A) Lysates prepared from control, F1.II:1 and F1.II:2 fibroblasts were probed for Trafficking Protein Particle Complex subunit 11 (TRAPPC11), LAMP1 and tubulin as a loading control. (B) Fibroblasts were infected with virus encoding VSVG–GFP ts045. The fusion protein was retained in the endoplasmic reticulum (ER) at 40°C overnight. The cells were then treated with cycloheximide and shifted to 32°C to release a synchronised wave of protein from the ER. Samples were collected at the indicated time points and a portion of the lysate was treated with endoglycosidase H (endo H). The protein was visualised by western blot analysis using an anti-GFP antibody. A representative blot is shown. (C) The data from three independent experiments described in (B) were quantitated and are displayed as ±SEM. Statistical significance was assessed using a Student's t-test. (D) The VSVG–GFP ts045 assay was performed as described in (B) except that the cells were fixed and stained for mannosidase II (man II) and GFP at the indicated time points. Scale bars are 50 μm. (E) Cells at the time points in (D) were quantified by measuring GFP immunoreactivity intensity in the Golgi region (defined by man II staining) compared with the total GFP immunoreactivity in the cell. For each time point, N ranges from 5 to 15.

defect and reduced mRNA levels of the regular splice product described above. In a previous study characterising the TRAPPC11 mutations p.G980R and p.A372_S429del, hyperglycosylation of lysosomal-associated membrane protein 1 (LAMP1) was demonstrated.[26] In contrast to that study, we found that LAMP1 was hypoglycosylated in both F1.II:1 and F1.II:2 (figure 3A). This result could reflect a membrane trafficking defect or a role for TRAPPC11 in protein glycosylation as recently reported.[27]

VSVG–GFP ts045 assay for monitoring the transport along the secretory pathway

Since TRAPPC11 has been implicated in endoplasmic reticulum (ER)-to-Golgi transport,[24 28] we next used an established assay to follow the movement of a protein from the ER, through the Golgi and on to its final destination, the plasma membrane.[29] The marker protein is a temperature-sensitive form of VSVG fused to GFP (VSVG–GFP ts045). At restrictive temperature, the protein is retained in the ER and as the temperature is lowered, in the presence of the protein synthesis inhibitor cycloheximide, there is a synchronised release of the protein from this compartment. Upon reaching the Golgi, the protein is eventually processed such that it becomes resistant to endoglycosidase H (endo H). Fibroblasts from unaffected and affected individuals were infected with a virus expressing VSVG–GFP ts045 and held at restrictive temperature overnight to allow accumulation of the protein in the ER. Samples were collected prior to the downshift in temperature and at time points up to 90 min after downshifting. A portion of the sample was treated with endo H to assess the location of the protein within the cell. As shown in figure 3B and C, at 40 min postdownshift, there was a slight delay in the acquisition of endo H resistance of the protein in the fibroblasts of affected individuals, suggesting a delay in the exit of the protein from the ER or a delay in traffic through the Golgi complex.

To distinguish between these two possibilities, cells were fixed at the same time points and the location of VSVG–GFP ts045 was assessed by immunofluorescence microscopy (figure 3D). Before downshifting of the temperature in the culture, the marker protein stains the cells in a diffuse reticular pattern consistent with ER localisation. By 20 and 40 min postdownshift, the marker protein colocalised with the Golgi marker mannosidase II in both affected and unaffected individuals. At the later time points, while the marker protein in unaffected individuals clearly separated from the Golgi marker and was found at the cell surface, a significant amount was retained in the Golgi in affected individuals. It is noteworthy that not all fibroblasts in the culture from affected individuals showed this phenotype. In fact, there were a number of cells that failed to show colocalisation between the Golgi marker and VSVG–GFP ts045 at the later time points (see below). Quantitation of the phenotype demonstrated a delay in the exit of the protein from the Golgi in affected individuals (figure 3E).

Time-lapse fluorescence microscopy to investigate dynamic events at the single-cell level

Since each time point in figure 3E represents a population of different cells at a given time point, we used time-lapse

microscopy to follow the movement of VSVG–GFP ts045 within the same cell over time (figure 4A–C and online supplementary movie 1). Consistent with the fixed cell data above, there was a clear delay in the release of the marker protein from the Golgi (quantified in figure 4D). In addition, we noted a slight delay in the arrival of the VSVG–GFP ts045 protein in the Golgi, suggesting there may either be two affected steps in membrane traffic or the delayed arrival in the Golgi may be a secondary consequence of reduced transport through the Golgi. Importantly, we identified two populations of cells within the culture from affected individuals: one showing the delays described above, representing ~70% of the cells, and a second with kinetics that were intermediate to those of unaffected cells, representing ~30% of the cells (figure 4C and online supplementary movie 2). This is consistent with the incomplete splicing defect suggested above and indicates that some cells may produce sufficient full-length TRAPPC11 to support near-normal membrane traffic.

Muscle biopsy

Histopathological evaluation of the muscle biopsy of patient F2. II:3 revealed mild dystrophic changes (figure 5A) like contraction, regeneration, degeneration, nuclear internalisation and fibrosis (figure 5B). In addition, many pathological immature myofibres were seen using the neonatal myosin staining (figure 5C). Based on immunostaining, α-sarcoglycan (α-SGC), delta-sarcoglycan (δ-SGC) and gamma-sarcoglycan (γ-SGC) were present at normal levels (figure 5D), whereas β-sarcoglycan (β-SGC) was deficient and conspicuously absent from focal patches (figure 5E). Other common structural proteins of muscle cell showed normal expression patterns and levels. Interestingly, there was also fibre-type grouping (figure 5F), which is specific for denervation with reinnervation seen in neuropathies and spinal muscular atrophy.[30]

DISCUSSION

Here, we investigated two apparently unrelated Turkish families each with two patients suffering from cerebral atrophy, global retardation, scoliosis, achalasia and alacrima. All patients have the same novel homozygous splice site mutation in *TRAPPC11*. The presence of a second mutation was excluded with MutationTaster2 analysis of all further variants found in the autozygous regions of family 2, although the possibility of an additional phenotype-influencing mutation cannot be completely ruled out. Triple A syndrome was initially assumed because the two symptoms alacrima and achalasia of this disease were present. In addition to these symptoms, patients showed more clinical abnormalities that are not described for triple A syndrome patients, although the missing feature of classical triple A syndrome (ie, adrenal insufficiency) may also develop at a later age.[31] We categorise this phenotype not as a new cause of triple A syndrome but rather as an expansion of the known *TRAPPC11* phenotype with myopathy, intellectual disability, alacrima and achalasia. Our patients carry the mutation c.1893 +3A>G, which leads to a partial loss of exon 18 (131 bp) resulting in a frameshift mutation (p.Val588Glyfs16*). The predicted shorter protein is estimated to be ~70 kDa in contrast to the full-length protein of ~130 kDa. mRNA quantification and western blot results suggest that the very low amount of intact *TRAPPC11* transcript in combination with an aberrant splicing product leads to the dysfunction of the protein and results in the observed phenotype of our patients. The reduced levels of

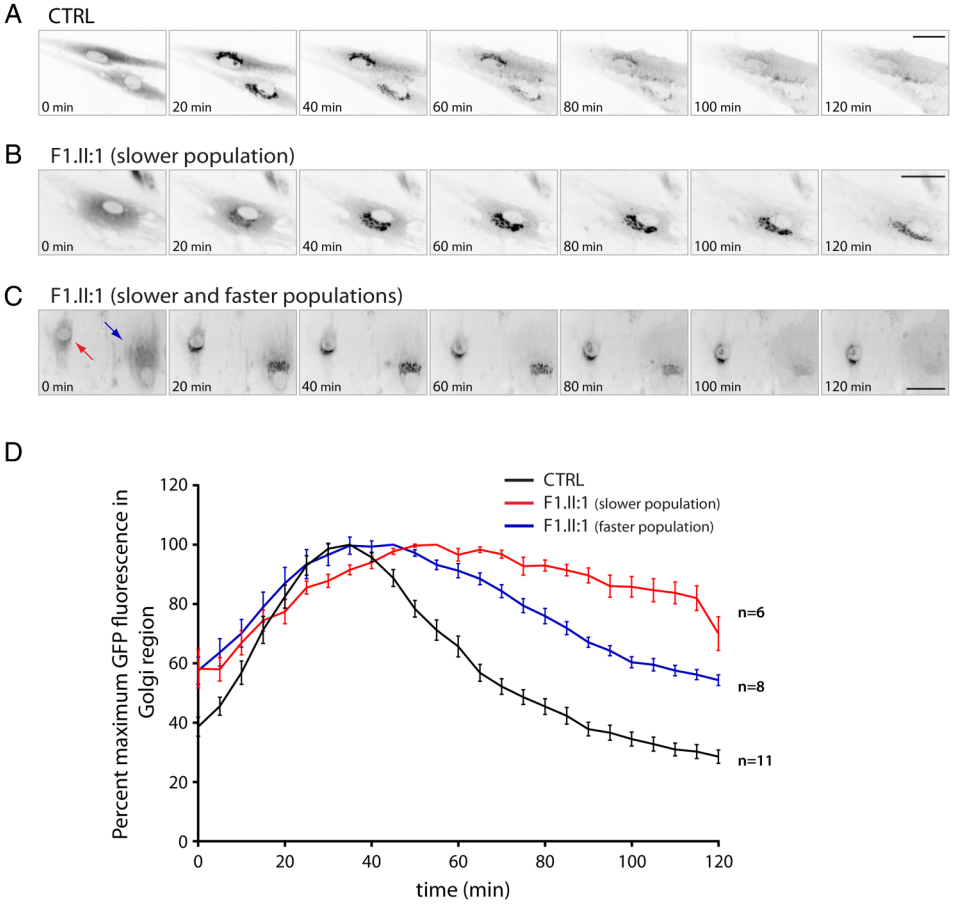

Figure 4 Live-cell imaging reveals two populations of fibroblasts derived from affected individuals. The vesicular stomatitis virus glycoprotein (VSVG)–GFP ts045 assay was performed as described in the legend to figure 3B except during the shift to 32°C, the cells were imaged every 30 s over a period of 120 min. Still images from the movies at the indicated time points are shown for control (A) and F1.II:1 (B and C). Scale bars are 50 μm. The full movies are shown in online supplementary movies 1 and 2. (D) The data from the live-cell imaging were quantified (n=6–11) by identifying the Golgi region at the time when the Golgi had a maximum fluorescence intensity (~30 min for the control and ~50 min for F1.II:1) and monitoring GFP fluorescence in the Golgi region for 120 min after the temperature shift. Data are shown as ±SEM.

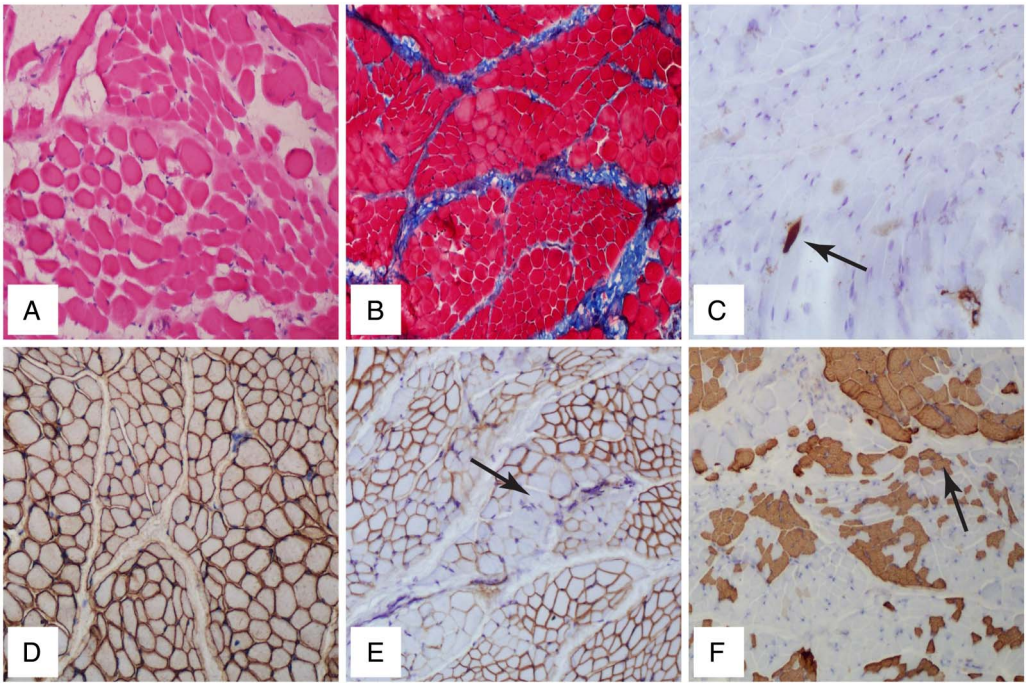

Figure 5 Immunohistochemical analyses reveal dystrophic changes in the affected individual F2.II:3. (A) A muscle biopsy from patient F2.II:3 was sectioned and stained with H&E to reveal the muscle fibres. Note the marked variation in fibre size and shape (200× magnification). (B) Muscle biopsy sections were stained with Masson's trichome and photographed at 100× magnification. There is marked fibrosis as seen by the distended blue-stained portions between the red-stained muscle fibres. (C) Muscle biopsy sections were stained with antibody against neonatal myosin and photographed at 200× magnification after 3,3′-diaminobenzidine (DAB) staining. There are a few immature fibres seen in the field (arrow). (D) Staining with anti-γ-sarcoglycan revealed normal sarcolemmal expression in muscle biopsy sections following DAB staining (200× magnification). (E) Staining with anti-β-sarcoglycan revealed the absence of focal sarcolemmal localisation of the protein following DAB staining (200× magnification) (arrow). (F) Staining of muscle biopsy sections with anti-MHCf showed marked fibre type grouping instead of the normal checkboard pattern following DAB staining (100× magnification) (arrow).

mutant *TRAPPC11* transcript are most likely due to nonsense-mediated RNA decay.[32]

The transport protein particle (TRAPP) is a multiprotein complex with several related but compositionally distinct forms. In yeast, these complexes function in a number of processes including ER-to-Golgi transport (TRAPP I), intra-Golgi and endosome-to-Golgi transport (TRAPP II) and autophagy (TRAPP III).[33] TRAPPC11 was identified as a component of the mammalian TRAPP III complex and has no recognisable yeast homologue.[24] The disruption of TRAPPC11 by viral insertional mutagenesis in zebrafish resulted in steatosis and cataracts, while RNAi depletion in HeLa cells and *Drosophila* S2 cells resulted in partial disassembly of the TRAPP complex and a defect in membrane transport in the early secretory pathway.[24 28 34]

Recently, a homozygous mutation in the *TRAPPC11* gene on chromosome 4q35 was identified in patients with autosomal recessive limb-girdle muscular dystrophy type 2S (LGMD2S) (MIM #615356), characterised by proximal muscle weakness resulting in gait abnormalities, scoliosis and scapular winging. A second homozygous mutation in which a small portion of the protein is deleted resulted in myopathy, ataxia, hyperkinetic movements and intellectual disability.[26] Furthermore, one Asian patient carrying a compound heterozygous mutation in *TRAPPC11* was described with congenital muscular dystrophy (CMD), progressive fatty liver and infantile-onset cataract.[35] From these reported cases, it can be concluded that the phenotype caused by *TRAPPC11* mutations includes myopathy and some variable accompanying features. Our patients differ from the other published cases in that they also have achalasia and alacrima, two typical symptoms of triple A syndrome. Usually, achalasia is an expression of neurological malfunction (loss of ganglion cells and myenteric nerves). Congenital alacrima is characterised by aplasia or hypoplasia of the lacrimal gland and can be depicted in MRI as bilateral lacrimal gland agenesis.[36]

We found that LAMP1 was hypoglycosylated in our patients' cells. This result may reflect the recently reported role of TRAPPC11 in protein glycosylation.[27] The glycoproteins LAMP1 and LAMP2 provide 50% of lysosomal membrane proteins.[37] They are coresponsible for maintaining lysosomal integrity, pH and catabolism of lysosomes and play an important role in the function of lysosomes. They are also involved in lysosomal exocytosis, movement of the lysosomes along microtubules and the fusion of phagosomes with lysosomes.[38] Acid hydrolases contained in the lysosomes mediate the degradation of cellular components and the defence against bacteria, viruses and toxic substances. Disturbances in these processes can have dramatic effects on cell metabolism. In contrast to our observation of LAMP1 hypoglycosylation, a previous study describing another *TRAPPC11* mutation demonstrated not only a reduction in the cellular levels of LAMP1 and LAMP2, but the proteins were observed in a higher molecular size region of the gel as compared with controls, suggesting that they might have a higher degree of glycosylation.[26] Taken together with these previous studies, our data suggest that the type of mutation, and not necessarily the cellular levels of TRAPPC11, can influence protein glycosylation. Alternatively, the defect in glycosylation may be related to a defect in membrane trafficking processes as was shown by the results in figures 3 and 4.

Disruption of Golgi structure has been reported in other neurodegenerative disorders such as amyotrophic lateral sclerosis,

Alzheimer's disease and Parkinson's disease.[39–41] It has been suggested that cellular stresses can affect Golgi morphology, possibly through a signalling pathway such as autophagy.[41] Thus, the connection between *TRAPPC11* mutations and the observed phenotypes may indeed be complex and need further investigation. Our results extend the cellular, phenotypic and genetic spectrum of TRAPPC11-related disorders and underline the essential role of TRAPPC11 in human physiology and cell homeostasis.

Author affiliations
[1]Klinik und Poliklinik für Kinder- und Jugendmedizin, Universitätsklinikum Carl Gustav Carus, Technische Universität Dresden, Dresden, Germany
[2]Department of Biology, Concordia University, Montreal, Quebec, Canada
[3]Pediatric Genetics Department, Ihsan Dogramaci Children's Hospital, Hacettepe University, Ankara, Turkey
[4]Department of Medical Genetics, Dr. Behçet Uz Children's Hospital, Izmir, Turkey
[5]Neuromuscular Diseases Centre, Tepecik Research Hospital, Izmir, Turkey
[6]Department of Neuropediatrics and NeuroCure Clinical Research Center, Charité-Universitätsmedizin Berlin, Berlin, Germany
[7]Department of Anatomy and Cell Biology, McGill University, Montreal, Quebec, Canada

Acknowledgements We are grateful to Kelley Moreman for providing the antimannosidase II antibody.

Contributors EU and FH phenotyped the patients. MSch and KK processed, analysed and validated the whole exome sequencing data. SK, DL and FR performed the Sanger sequencing. DL performed RNA and microsatellite analysis. MPM and KP performed western blotting, VSVG–GFP ts045 assay, fluorescence and time-lapse microscopy. GD performed the immunohistochemistry. KK, MPM, KP, RJ and MSa analysed and interpreted the data. AH, MSa and KK supervised the work and obtained funding support. KK and MSa wrote the manuscript. All authors read the final version of the manuscript and gave their permission for publication.

Funding This work was supported by a DFG grant HU 895/5-1 and HU 895/5-2 (Clinical Research Unit 252) to AH, SFB 665 TP C4 to MSch, a Canadian Institutes for Health Research grant and a Natural Sciences and Engineering Research Council grant to MSa.

Competing interests None declared.

Patient consent Parental consent obtained.

Ethics approval Local ethics review board (Medical Faculty, Technical University Dresden; EK820897).

Provenance and peer review Not commissioned; externally peer reviewed.

REFERENCES

1 Allgrove J, Clayden GS, Grant DB, Macaulay JC. Familial glucocorticoid deficiency with achalasia of the cardia and deficient tear production. *Lancet* 1978;1:1284–6.
2 Huebner A, Kaindl AM, Braun R, Handschug K. New insights into the molecular basis of the triple A syndrome. *EndocrRes* 2002;28:733–9.
3 Tullio-Pelet A, Salomon R, Hadj-Rabia S, Mugnier C, De Laet MH, Chaouachi B, Bakiri F, Brottier P, Cattolico L, Penet C, Begeot M, Naville D, Nicolino M, Chaussain JL, Weissenbach J, Munnich A, Lyonnet S. Mutant WD-repeat protein in triple-A syndrome. *Nat Genet* 2000;26:332–5.
4 Handschug K, Sperling S, Yoon SJ, Hennig S, Clark AJ, Huebner A. Triple A syndrome is caused by mutations in AAAS, a new WD-repeat protein gene. *Hum Mol Genet* 2001;10:283–90.
5 Cronshaw JM, Krutchinsky AN, Zhang W, Chait BT, Matunis MJ. Proteomic analysis of the mammalian nuclear pore complex. *J Cell Biol* 2002;158:915–27.
6 Cronshaw JM, Matunis MJ. The nuclear pore complex protein ALADIN is mislocalized in triple A syndrome. *Proc Natl Acad Sci USA* 2003;100:5823–7.
7 Krumbholz M, Koehler K, Huebner A. Cellular localization of 17 natural mutant variants of ALADIN protein in triple A syndrome—shedding light on an unexpected splice mutation. *Biochem Cell Biol* 2006;84:243–9.
8 Kind B, Koehler K, Krumbholz M, Landgraf D, Huebner A. Intracellular ROS level is increased in fibroblasts of triple A syndrome patients. *J Mol Med* 2010;88:1233–42.
9 Jühlen R, Idkowiak J, Taylor AE, Kind B, Arlt W, Huebner A, Koehler K. Role of ALADIN in human adrenocortical cells for oxidative stress response and steroidogenesis. *PLoS ONE* 2015;10:e0124582.
10 Koehler K, Malik M, Mahmood S, Giesselmann S, Beetz C, Hennings JC, Huebner AK, Grahn A, Reunert J, Nurnberg G, Thiele H, Altmuller J, Nurnberg P, Mumtaz R, Babovic-Vuksanovic D, Basel-Vanagaite L, Borck G, Bramswig J, Muhlenberg R, Sarda P, Sikiric A, nyane-Yeboa K, Zeharia A, Ahmad A, Coubes C, Wada Y, Marquardt T, Vanderschaeghe D, Van SE, Kurth I, Huebner A, Hubner CA. Mutations in GMPPA cause a glycosylation disorder characterized by intellectual disability and autonomic dysfunction. *Am J Hum Genet* 2013;93:727–34.
11 Reschke F, Köhler K, Landgraf D, Susann K, Utine E, Hazan F, Hübner A. A novel mutation of the TRAPPC11 gene causes a disease with cerebral atrophy, global retardation, therapy refractory seizures, achalasia, and alacrima: a triple a-like syndrome. *Neuropediatrics* 2014;45:fp020.
12 Vissing J. Limb girdle muscular dystrophies: classification, clinical spectrum and emerging therapies. *Curr Opin Neurol* 2016;29:635–41.
13 Vuillaumier-Barrot S, Quijano-Roy S, Bouchet-Seraphin C, Maugenre S, Peudenier S, Van den Bergh P, Marcorelles P, Avila-Smirnow D, Chelbi M, Romero NB, Carlier RY, Estournet B, Guicheney P, Seta N. Four Caucasian patients with mutations in the fukutin gene and variable clinical phenotype. *Neuromuscul Disord* 2009;19:182–8.
14 Balci B, Uyanik G, Dincer P, Gross C, Willer T, Talim B, Haliloglu G, Kale G, Hehr U, Winkler J, Topaloğlu H. An autosomal recessive limb girdle muscular dystrophy (LGMD2) with mild mental retardation is allelic to Walker-Warburg syndrome (WWS) caused by a mutation in the POMT1 gene. *Neuromuscul Disord* 2005;15:271–5.
15 van Reeuwijk J, Janssen M, van den Elzen C, Beltran-Valero de Bernabé D, Sabatelli P, Merlini L, Boon M, Scheffer H, Brockington M, Muntoni F, Huynen MA, Verrips A, Walsh CA, Barth PG, Brunner HG, van Bokhoven H. POMT2 mutations cause alpha-dystroglycan hypoglycosylation and Walker-Warburg syndrome. *J Med Genet* 2005;42:907–12.
16 Clement E, Mercuri E, Godfrey C, Smith J, Robb S, Kinali M, Straub V, Bushby K, Manzur A, Talim B, Cowan F, Quinlivan R, Klein A, Longman C, McWilliam R, Topaloglu H, Mein R, Abbs S, North K, Barkovich AJ, Rutherford M, Muntoni F. Brain involvement in muscular dystrophies with defective dystroglycan glycosylation. *Ann Neurol* 2008;64:573–82.
17 Brockington M, Blake DJ, Prandini P, Brown SC, Torelli S, Benson MA, Ponting CP, Estournet B, Romero NB, Mercuri E, Voit T, Sewry CA, Guicheney P, Muntoni F. Mutations in the fukutin-related protein gene (FKRP) cause a form of congenital muscular dystrophy with secondary laminin alpha2 deficiency and abnormal glycosylation of alpha-dystroglycan. *Am J Hum Genet* 2001;69:1198–209.
18 Longman C, Brockington M, Torelli S, Jimenez-Mallebrera C, Kennedy C, Khalil N, Feng L, Saran RK, Voit T, Merlini L, Sewry CA, Brown SC, Muntoni F. Mutations in the human LARGE gene cause MDC1D, a novel form of congenital muscular dystrophy with severe mental retardation and abnormal glycosylation of alpha-dystroglycan. *Hum Mol Genet* 2003;12:2853–61.
19 Carss KJ, Stevens E, Foley AR, Cirak S, Riemersma M, Torelli S, Hoischen A, Willer T, van Scherpenzeel M, Moore SA, Messina S, Bertini E, Bönnemann CG, Abdenur JE, Grosmann CM, Kesari A, Punetha J, Quinlivan R, Waddell LB, Young HK, Wraige E, Yau S, Brodd L, Feng L, Sewry C, MacArthur DG, North KN, Hoffman E, Stemple DL, Hurles ME, van Bokhoven H, Campbell KP, Lefeber DJ, UK10K Consortium, Lin Y-Y, Muntoni F. Mutations in GDP-mannose pyrophosphorylase B cause congenital and limb-girdle muscular dystrophies associated with hypoglycosylation of α-dystroglycan. *Am J Hum Genet* 2013;93:29–41.
20 von Renesse A, Petkova MV, Lützkendorf S, Heinemeyer J, Gill E, Hübner C, von Moers A, Stenzel W, Schuelke M. POMK mutation in a family with congenital muscular dystrophy with merosin deficiency, hypomyelination, mild hearing deficit and intellectual disability. *J Med Genet* 2014;51:275–82.
21 Seelow D, Schuelke M. HomozygosityMapper2012—bridging the gap between homozygosity mapping and deep sequencing. *Nucleic Acids Res* 2012;40:W516–20.
22 Schwarz JM, Cooper DN, Schuelke M, Seelow D. MutationTaster2: mutation prediction for the deep-sequencing age. *Nat Methods* 2014;11:361–2.
23 Schuelke M. An economic method for the fluorescent labeling of PCR fragments. *Nat Biotechnol* 2000;18:233–4.
24 Scrivens PJ, Noueihed B, Shahrzad N, Hul S, Brunet S, Sacher M. C4orf41 and TTC-15 are mammalian TRAPP components with a role at an early stage in ER-to-Golgi trafficking. *Mol Biol Cell* 2011;22:2083–93.
25 Lal D, Neubauer BA, Toliat MR, Altmüller J, Thiele H, Nürnberg P, Kamrath C, Schänzer A, Sander T, Hahn A, Nothnagel M. Increased Probability of Co-Occurrence of Two Rare Diseases in Consanguineous Families and Resolution of a Complex Phenotype by Next Generation Sequencing. *PLoS ONE* 2016;11:e0146040.
26 Bögershausen N, Shahrzad N, Chong JX, von Kleist-Retzow J-C, Stanga D, Li Y, Bernier FP, Loucks CM, Wirth R, Puffenberger EG, Hegele RA, Schreml J, Lapointe G, Keupp K, Brett CL, Anderson R, Hahn A, Innes AM, Suchowersky O, Mets MB, Nürnberg G, McLeod DR, Thiele H, Waggoner D, Altmüller J, Boycott KM, Schoser B, Nürnberg P, Ober C, Heller R, Parboosingh JS, Wollnik B, Sacher M, Lamont RE. Recessive TRAPPC11 Mutations Cause a Disease Spectrum of Limb Girdle Muscular Dystrophy and Myopathy with Movement Disorder and Intellectual Disability. *Am J Hum Genet* 2013;93:181–90.
27 DeRossi C, Vacaru A, Rafiq R, Cinaroglu A, Imrie D, Nayar S, Baryshnikova A, Milev MP, Stanga D, Kadakia D, Gao N, Chu J, Freeze HH, Lehrman MA, Sacher M, Sadler KC. trappc11 is required for protein glycosylation in zebrafish and humans. *Mol Biol Cell* 2016;27:1220–34.

28 Wendler F, Gillingham AK, Sinka R, Rosa-Ferreira C, Gordon DE, Franch-Marro X, Peden AA, Vincent J-P, Munro S. A genome-wide RNA interference screen identifies two novel components of the metazoan secretory pathway. *EMBO J* 2010;29:304–14.
29 Scales SJ, Pepperkok R, Kreis TE. Visualization of ER-to-Golgi transport in living cells reveals a sequential mode of action for COPII and COPI. *Cell* 1997;90:1137–48.
30 Heffner RR, Moore D, Balos LL. Muscle Biopsy in Neuromuscular Diseases. In: Mills SE, ed. *Sternberg's diagnostic surgical pathology*. 6th edition. Philadelphia, PA: Wolters Kluwer, 2015:117–118.
31 Huebner A, Kaindl AM, Knobeloch KP, Petzold H, Mann P, Koehler K. The triple A syndrome is due to mutations in ALADIN, a novel member of the nuclear pore complex. *Endocr Res* 2004;30:891–9.
32 Khajavi M, Inoue K, Lupski JR. Nonsense-mediated mRNA decay modulates clinical outcome of genetic disease. *Eur J Hum Genet* 2006;14:1074–81.
33 Brunet S, Sacher M. In sickness and in health: the role of TRAPP and associated proteins in disease. *Traffic Cph Den* 2014;15:803–18.
34 Sadler KC, Amsterdam A, Soroka C, Boyer J, Hopkins N. A genetic screen in zebrafish identifies the mutants vps18, nf2 and foie gras as models of liver disease. *Dev Camb Engl* 2005;132:3561–72.
35 Liang WC, Zhu W, Mitsuhashi S, Noguchi S, Sacher M, Ogawa M, Shih H-H, Jong Y-J, Nishino I. Congenital muscular dystrophy with fatty liver and infantile-onset cataract caused by TRAPPC11 mutations: broadening of the phenotype. *Skelet Muscle* 2015;5:29.
36 Li W, Gong C, Qi Z, Wu DI, Cao B. Identification of AAAS gene mutation in Allgrove syndrome: A report of three cases. *Exp Ther Med* 2015;10:1277–82.
37 Eskelinen EL. Roles of LAMP-1 and LAMP-2 in lysosome biogenesis and autophagy. *Mol Aspects Med* 2006;27:495–502.
38 Schwake M, Schröder B, Saftig P. Lysosomal membrane proteins and their central role in physiology. *Traffic Cph Den* 2013;14:739–48.
39 Haase G, Rabouille C. Golgi Fragmentation in ALS Motor Neurons. New Mechanisms Targeting Microtubules, Tethers, and Transport Vesicles. *Front Neurosci* 2015;9:448.
40 Joshi G, Bekier ME, Wang Y. Golgi fragmentation in Alzheimer's disease. *Front Neurosci* 2015;9:340.
41 Machamer CE. The Golgi complex in stress and death. *Front Neurosci* 2015;9:421.